

Diode-pumped continuous-wave and passively mode-locked Yb:GSO laser

Wenxue Li, Haifeng Pan, Liang'en Ding, and Heping Zeng

Key Laboratory of Optical and Magnetic Resonance Spectroscopy, and Department of Physics,
East China Normal University, Shanghai 200062, P. R. China

Guangjun Zhao, Chengfeng Yan, Liangbi Su, and Jun Xu

Shanghai Institute of Optics and Fine Mechanics, Chinese Academy of Sciences, Shanghai 201800, P. R. China
hpzeng@phy.ecnu.edu.cn

Abstract: We report on both continuous-wave and passively mode-locked laser actions of a new ytterbium-doped laser crystal Yb:Gd₂SiO₅ (Yb:GSO) under high-power diode-end-pumping. Due to the anisotropic and compact crystal structure, Yb:GSO exhibits a large manifold splitting of Yb³⁺ ions, and a Yb:GSO laser can be operated efficiently with negligible reabsorption losses at emission wavelengths. In the continuous-wave operation, a Yb:GSO laser was operated with a slope efficiency of 49% near 1094 nm—the longest laser wavelength achieved for Yb³⁺ lasers. Passive mode locking was obtained with a semiconductor saturable-absorber mirror. At a pump power of 6.23 W, a maximum average output power of 638 mW was obtained with the repetition rate of 145.5 MHz.

©2006 Optical Society of America

OCIS codes: (140.5680) Rare earth and transition metal solid-state lasers; (140.3480) Lasers, diode-pumped; (140.4050) Mode-locked lasers

References and links

1. S. Chénais, F. Druon, F. Balembois, G. Lucas-Leclin, P. Georges, A. Brun, M. Zavelani-Rossi, F. Augé, J.-P. Chambaret, G. Aka, and D. Vivien, "Multiwatt, tunable, diode-pumped CW Yb:GdCOB laser," *Appl. Phys. B* **72**, 389-393 (2001).
2. F. Druon, S. Chénais, P. Raybaut, F. Balembois, P. Georges, R. Gaumé, G. Aka, B. Viana, S. Mohr, and D. Kopf, "Diode-pumped YbSr₃Y(BO₃)₃ femtosecond laser," *Opt. Lett.* **27**, 197-199 (2002).
3. F. Brunner, T. Südmeyer, E. Innerhofer, F. Morier-Genoud, R. Paschotta, V. E. Kisel, V. G. Scherbitsky, N. V. Kuleshov, J. Gao, K. Contag, A. Giesen, and U. Keller, "240-fs pulses with 22-W average power from a mode-locked thin-disk Yb:KY(WO₄)₂ laser," *Opt. Lett.* **27**, 1162-1164 (2002).
4. F. Brunner, G. J. Spuheler, J. Aus der Au, L. Krainer, F. Morier-Genoud, R. Paschotta, N. Lichtenstein, S. Weiss, C. Harder, A. A. Lagatsky, A. Abdolvand, N. V. Kuleshov, and U. Keller, "Diode-pumped femtosecond Yb:KGd(WO₄)₂ laser with 1.1-W average power," *Opt. Lett.* **25**, 1119-1121 (2000).
5. S. A. Payne, L. K. Smith, L. D. DeLoach, W. L. Kway, J. B. Tassano, and W. F. Krupke, "Laser, optical, and thermomechanical properties of Yb-doped fluorapatite," *IEEE J. Quantum Electron.* **30**, 170-179 (1994).
6. F. Druon, S. Chénais, P. Raybaut, F. Balembois, P. Georges, R. Gaumé, P. H. Haumesser, B. Viana, D. Vivien, S. Dhellemmes, V. Ortiz, and C. Larat, "Apatite-structure crystal, Yb³⁺:SrY₄(SiO₄)₃O, for the development of diode-pumped femtosecond lasers," *Opt. Lett.* **27**, 1914-1916 (2002).
7. P. Lacovara, H. K. Choi, C. A. Wang, R. L. Aggarwal, and T. Y. Fan, "Room-temperature diode-pumped Yb:YAG laser," *Opt. Lett.* **16**, 1089-1091 (1991).
8. S. Chénais, F. Druon, F. Balembois, P. Georges, A. Brenier, and G. Boulon, "Diode-pumped Yb:GGG laser: comparison with Yb:YAG," *Opt. Mater.* **22**, 99-106 (2003).
9. M. Jacquemet, C. Jacquemet, N. Janel, F. Druon, F. Balembois, P. Georges, J. Petit, B. Viana, D. Vivien, and B. Ferrand, "Efficient laser action of Yb:LSO and Yb:YSO oxyorthosilicates crystals under high-power diode pumping," *Appl. Phys. B* **80**, 171-176 (2005).
10. F. Thibault, D. Pelenc, F. Druon, and P. Georges, "Very efficient diode-pumped Yb³⁺:Y₂SiO₅ and Yb³⁺:Lu₂SiO₅ femtosecond laser," *Conference on Lasers and Electro-Optics Europe 2005, CFB1*.
11. A. Lucca, M. Jacquemet, F. Druon, F. Balembois, P. Georges, P. Camy, J. L. Doualan, and R. Moncorge, "High-power tunable diode-pumped Yb³⁺:CaF₂ laser," *Opt. Lett.* **29**, 1879-1881 (2004).

12. A. Lucca, G. Debourg, M. Jacquemet, F. Druon, F. Balembois, P. Georges, P. Camy, J. L. Doualan, and R. Moncorgé, "High power diode-pumped Yb³⁺:CaF₂ femtosecond laser," *Opt. Lett.* **29**, 2767–2769 (2004).
13. J. Kong, D.Y. Tang, J. Lu, K. Ueda, H. Yagi, and T. Yanagitani, "Diode-end-pumped 4.2-W continuous-wave Yb:Y₂O₃ ceramic laser," *Opt. Lett.* **29**, 1212–1214 (2004).
14. K. Petermann, L. Fornasiero, E. Mix, and V. Peters, "High melting sesquioxides: crystal growth, spectroscopy, and laser experiments," *Opt. Mater.* **19**, 67–71 (2002).
15. A. Courjaud, R. Maleck-Rassoul, N. Deguil, C. Hönninger, and F. Salin, "Diode pumped multikilohertz femtosecond amplifier," in *OSA Trends in Optics and Photonics, Advanced Solid-State Lasers Vol. 68*, pp. 121–123 (2002).
16. H. Liu, J. Nees, and G. Mourou, "Directly diode-pumped YbKY(WO₄)₂ regenerative amplifiers," *Opt. Lett.* **27**, 722–724 (2002).
17. P. Raybaut, F. Druon, F. Balembois, P. Georges, R. Gaumé, B. Viana, and D. Vivien, "Directly diode-pumped Yb³⁺:SrY₄(SiO₄)₃O regenerative amplifier," *Opt. Lett.* **28**, 2195–2197 (2003).
18. P. Haumesser, R. Gaumé, B. Viana, and D. Vivien, "Determination of laser parameters of ytterbium-doped oxide crystalline materials," *J. Opt. Soc. Am. B* **19**, 2365–2375 (2002).
19. C. Hönninger, R. Paschotta, F. Morier-Genoud, M. Moser, and U. Keller, "Q-switching stability limits of continuous-wave passive mode locking," *J. Opt. Soc. Am. B* **16**, 46–56 (1999).

1. Introduction

In the past few years, there has been growing interest in ytterbium-doped materials as attractive laser gain media for efficient, simple, and compact directly diode-pumped solid-state lasers near 1 μm . Ytterbium-doped crystals usually exhibit weak absorption lines between 900 and 950 nm, a strong zero-line absorption peak around 980 nm, and broadband emission transitions between 1010 and 1090 nm, typically with high emission cross sections between 1020 and 1060 nm. The strong zero-line absorption bands are well matched to the high-power InGaAs laser diodes of approximately 980 nm. The spectroscopic properties and the simple electronic-level scheme of Yb³⁺ ions favor quite encouraging elimination of undesired effects, such as excited-state absorption, cross relaxation, upconversion, and concentration quenching. In particular, relatively low intrinsic quantum defects (generally less than 10%) of Yb³⁺ ions results in reduction of thermal load. Efficient laser operations have already been demonstrated in many ytterbium-doped crystals, such as borate Yb:GdCOB and Yb:BOYS [1,2], tungstates Yb:KYW and Yb:KGW [3,4], fluoroapatites Yb:S-FAP [5], silicate oxyapatite Yb:SYS [6], garnet Yb:YAG and Yb:GGG [7,8], oxyorthosilicates Yb:YSO and Yb:LSO [9,10], fluoride Yb:CaF₂ [11,12], or sesquioxides Yb:Y₂O₃, Yb:Lu₂O₃, and Yb:Sc₂O₃ [13,14]. Numerous ytterbium-doped crystals have been recognized in recent years as very attractive active media for diode-pumped femtosecond laser oscillators and amplifiers [15,16,17].

So far, there still exist no "ideal" ytterbium-doped crystals with the combination of merits such as broad amplification bandwidth, relatively large laser cross section, good thermal conductivity, low quantum defect, and ease of growth. In the high-power laser domain, a crucial issue is to control heat production in the ytterbium-doped gain media. Numerous ytterbium-doped materials have a relatively low thermal conductivity. Yb:YAG possesses a high thermal conductivity but a narrow and unpolarized emission band, and ytterbium sesquioxides have a high thermal conductivity but a relatively narrow emission spectrum, and they are somewhat difficult to grow. On the other hand, a main drawback of current Yb³⁺ lasers comes from the quasi-three-level operating scheme. Depending on the host matrices, the splitting of the fundamental manifold ²F_{7/2} of Yb³⁺ in a large number of ytterbium-doped crystals is typically a few hundreds of cm⁻¹, and therefore the energy difference between the fundamental pumping level and the terminal laser level is comparable to the thermal energy k_BT at room temperature. Thermal populating of the terminal laser level causes strong reabsorption at the emission wavelengths, resulting in a high laser pumping threshold power. It is still a challenge to get ytterbium-doped crystals with sufficiently large splittings of the fundamental manifold ²F_{7/2} of Yb³⁺ so that the corresponding Yb³⁺ lasers work in a quasi-four-level scheme as the Nd³⁺ counterparts. Recently, Yb-doped oxyorthosilicates Yb:YSO and

Yb:LSO have been demonstrated to exhibit large emission spectra, large ground-state splittings, and high thermal conductivities [9,10].

In this paper, we demonstrate efficient laser action of a new ytterbium-doped oxyorthosilicate crystal, Yb:GSO. Since the GSO is more anisotropic and has a more compact structure than YSO or LSO due to the replacement of yttrium or lutetium ions with gadolinium ions in the oxyorthosilicate host matrix, Yb³⁺ ions in the GSO host experience quite stronger crystal-field interactions that cause a larger manifold splitting. The overall splitting of the ²F_{7/2} manifold reaches up to 1067 cm⁻¹, which is to the best of our knowledge the largest ground-state splitting. Such a large splitting of the fundamental manifold promises Yb:GSO lasers of low pump threshold, since reabsorption losses at emission wavelengths can be decreased due to low thermal population of the terminal laser level. In addition, the weak mass difference between gadolinium and ytterbium doping makes a weak decrease in thermal conductivity of the GSO, and therefore Yb:GSO, even with a high doping concentration, possesses a promising high conductivity. The emission bandwidth of Yb:GSO reaches as broad as ~72 nm, which is much broader than that of Yb:YAG. A Yb:GSO laser may exhibit a large tunability. In this work, the room-temperature absorption and emission spectra of Yb:GSO are studied, and diode-pumped cw and passively mode-locked Yb:GSO lasers are demonstrated. Since Yb:GSO possesses the largest branching ratio and the largest emission cross section for the emission band at the longest wavelength (~1088 nm), the Yb:GSO laser around this band becomes the most efficient one with the lowest threshold. We realized a cw Yb:GSO laser at 1094 nm, which is to the best of our knowledge the longest laser wavelength achieved for Yb³⁺ lasers. With a semiconductor saturable absorption mirror (SESAM) to launch passive mode locking, we obtained a cw mode-locked (CML) Yb:GSO laser.

2. Spectral properties of Yb:GSO

The Yb:GSO single crystal was grown by the Czochralski method in inductively heated iridium crucibles under nitrogen-ambient atmosphere. The charges were prepared from Gd₂O₃ (4N), Yb₂O₃ (4N), and SiO₂ (5N). The starting materials were fired at 1000 °C for more than 10 h to remove moisture, and then pressed into pellets and sintered at 1200 °C before being loaded into the iridium crucible. The seed crystals were oriented at 60° relative to the [0 1 0] axis. Optical absorption spectra of the as-grown Yb:GSO single crystal was recorded by a Jasco V-570 UV/VIS/NIR spectrophotometer at room temperature. The luminescence spectra were obtained with a Triax550 spectrofluorimeter under 940 nm laser diode excitation.

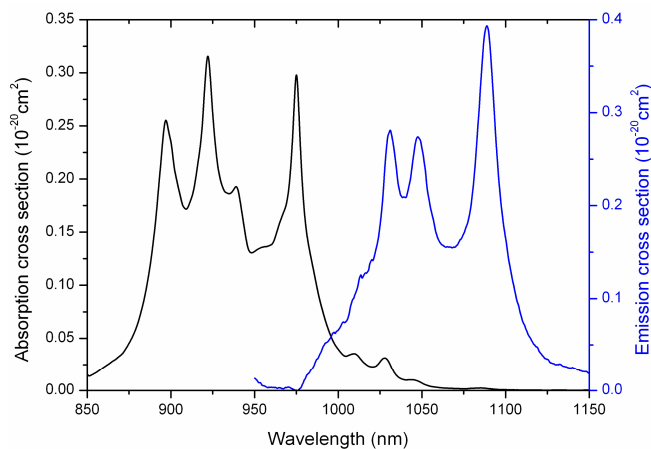


Fig. 1. Room-temperature absorption and emission spectra of the Yb:GSO laser crystal.

The fluorescence decay curves were recorded and averaged by a computer-controlled transient digitizer. The room-temperature absorption and emission spectra of the 10 at.% Yb³⁺-doped GSO crystal, shown in Fig. 1, are greatly different from those of Yb:YSO or Yb:LSO (see Fig. 2 in Ref. 9). The fluorescence lifetime of Yb:GSO was determined as 1.1 ms at 1088 nm. Since the reabsorption loss is negligible at 1088 nm, the fluorescence lifetime can be considered as radiative lifetime. We can therefore determine the emission cross sections of Yb:GSO by using the Fuchtbauer-Ladenburg relationship [18]. The absence of the zero-phonon emission line is due to the strong reabsorption loss and low emission cross section. The absorption spectrum is mainly composed of four strong bands around 897, 922, 940, and 976 nm. The absorption peak of approximately 976 nm belongs to the zero-line transition between the lowest levels of ²F_{7/2} and ²F_{5/2} manifolds. Other transition bands correspond to the typical transitions from the ground state ²F_{7/2} to the other sublevels of ²F_{5/2} of Yb³⁺. The absorption bandwidth of Yb³⁺ in a GSO host is much larger than that in Yb:YAG. The absorption bandwidth of Yb:GSO at 940 and 976 nm is about 16 and 19 nm, respectively. Its broadband is well adapted for diode-pumping with commercially available high-power InGaAs laser diodes. The absorption cross sections at 940 and 976 nm have been estimated at 0.20×10^{-20} and 0.31×10^{-20} cm², respectively.

The emission spectrum mainly includes four bands centered around 1013, 1031, 1048, and 1088 nm, whose emission cross sections are 0.20×10^{-20} , 0.39×10^{-20} , 0.31×10^{-20} and 0.42×10^{-20} cm², respectively. Those emission bands exhibit a very small quantum defect as the zero-line absorption transition is used for pumping, which as a consequence, reduces the heat deposition into the crystal. Particularly, Yb:GSO has a quite broad emission bandwidth up to ~72 nm, which is much broader than that of Yb:YAG. Among all the four emission bands, the emission band at 1088 nm possesses the largest emission cross section. This is contrary to other ytterbium-doped oxyorthosilicates such as Yb:YSO and Yb:LSO, wherein the emission band at the longest wavelengths (around 1080 nm in Yb:YSO or Yb:LSO) has the smallest emission cross section. As a result, laser output around 1088 nm becomes the most efficient one with the lowest threshold.

Large splitting of the fundamental manifold is of critical importance to limit the thermal population of the terminal laser level and then to decrease the laser threshold in the quasi-three-level laser operation. As previously said, a quasi-four-level laser operating scheme for Yb³⁺ can be expected in the crystal hosts with large splitting of the fundamental manifold. According to the absorption and emission in Fig. 1, one can estimate that the splitting of the ground-state manifold ²F_{7/2} in Yb:GSO is about 1067 cm⁻¹, which is much larger than those in Yb:YSO and Yb:LSO, and even Yb:GdCOB of 1003 cm⁻¹ [1].

In the GSO host lattice, there are two nonequivalent crystallographic sites of Gd³⁺, which are coordinated with 7 and 9 oxygen atoms, respectively. Accordingly, there exist two substitution sites for rare-earth-ion doping, one of which has larger manifold splitting (II) and another relatively smaller (I). The small emission cross section of the band at 1080 nm in Yb:YSO or Yb:LSO indicates that a low proportion of Yb³⁺ ions enters substitution site II, while the occurrence of the largest emission cross section of the emission band at 1088 nm suggests that a high proportion of Yb³⁺ ions in the GSO host matrices enters substitution site I. This is most favorable for low-threshold and high-efficiency laser operating around this emission band.

The spectroscopic and laser difference of the ytterbium-doped oxyorthosilicate crystals can be qualitatively understood by noting the difference of the crystal structures. The crystal structure of Y₂SiO₅ and Lu₂SiO₅ belongs to the end-centered monoclinic I2/a space group. Hereby, the (SiO₄) and (OY₄) or (OLu₄) tetrahedra share edges and form chains interconnected by isolated (SiO₄) tetrahedra. The structure of Gd₂SiO₅ belongs to the primitive monoclinic space group P2₁/c and is composed of a two-dimensional network of corner-linked (OGd₄) tetrahedra where the (SiO₄) tetrahedra are packed. Accordingly, Gd₂SiO₅ is more anisotropic and has more compact structure than YSO or LSO, which results in larger manifold splitting for Yb³⁺.

3. Experimental setup

In the first part of the experiments, we tested cw laser operation of 5 at.% and 10 at.%-doped Yb:GSO with a simple cavity configuration, as schematically shown in Fig. 2. The laser cavity consists of two mirrors (M_1 and OC), where M_1 (radius-of-curvature: ROC=100 mm) is antireflection-coated at 974 nm and high-reflection coated in a broad band from 1020 to 1120 nm, and OC is the output coupler with different transmission ($T=2.5\%$, $T=5.5\%$ and $T=10\%$). The overall cavity length is about 5 cm. All the Yb:GSO crystals are antireflection-coated with the gain length of 1.5 mm (5 mm \times 6 mm in size). The crystal is end-pumped by a fiber-coupled laser diode with the emission wavelength at 974 nm controlled by a temperature regulation. The diameter and numerical aperture of the fiber core are 400 μm and 0.22, respectively. The pump laser beam is focused by a series of lenses with a pump spot about 400 μm on the Yb:GSO crystal. To efficiently remove the generated heat during the experiment, we wrapped the crystal with indium foil and fixed it tightly in a water-cooled copper heat sink. The temperature of laser crystal was controlled at 14°C to lower the laser threshold.

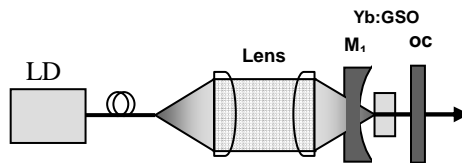


Fig. 2. Schematic of Yb:GSO cw laser cavity.

In a passively mode-locked operation, we employed a folded resonator, as schematically shown in Fig. 3. The laser cavity consists of a SESAM and three mirrors: an input concave mirror M_1 (ROC=100 mm) with high transmission at 974 nm and high reflection in a broad band from 1020 to 1120 nm, two folded concave mirrors M_2 ($R=500$ mm) and M_3 (ROC=100 mm) with high reflection in a broad band from 1020 to 1120 nm, and an output coupler (OC) flat mirror with a transmission of 2.5%. The length between M_1 and M_2 is about 350 mm, while M_2 and OC are separated by 233 mm, and the length between OC and SESAM is 451 mm. The total cavity length is added up to 1034 mm. The central wavelength of the SESAM (BATOP GmbH, Germany) in our experiment is 1064 ± 5 nm. Around the central wavelength, the saturation fluence is 70 $\mu\text{J}/\text{cm}^2$, the saturation absorption is 2.0%, while the nonsaturable loss is less than 0.3%. And the relaxation time is as short as 20 ps. The SESAM was mounted

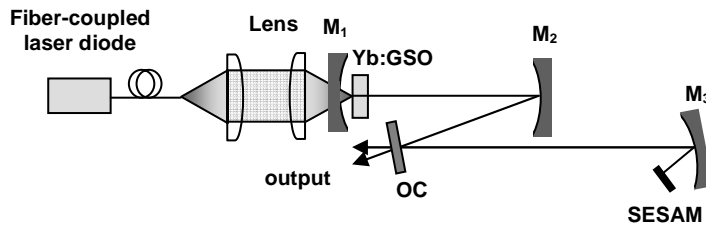


Fig. 3. Schematic of a Yb:GSO laser passively mode locked with a SESAM. M_1 , cavity mirror; M_2 , M_3 , folding mirrors; OC, output coupler.

on a thermoelectric device. The laser cavity was designed to get a beam diameter of 240 μm on the crystal and 80 μm on the SESAM, respectively. The mode-locked pulse train was

detected by a fast photodiode with a rising time of less than 200 ps and recorded with a digital storage oscilloscope. The resonator was carefully designed to suppress the strong tendency toward Q-switching or Q-switched mode-locking, which is a particularly severe issue for Yb-doped materials [19].

4. Results and discussion

In the case of cw laser operation, as expected, the preferred laser of Yb:GSO crystal was operated at 1094 nm under direct diode-pumping at 974 nm. According to the emission spectrum, laser action may occur around the strong emission bands of 1031, 1048, and 1088 nm. In addition to the smallest thermal populating of the terminal laser level, which brings about smallest reabsorption losses, the longest emission band possesses the strongest emission cross section. Accordingly, the Yb:GSO laser oscillates around the longest emission band. The Yb:GSO laser characteristics can be compared with those of Yb:YSO and Yb:LSO [9,10]. The emission spectra of Yb:YSO and Yb:LSO are mainly composed of three bands around 1000, 1050 and 1080 nm. In either Yb:YSO or Yb:LSO, the largest emission cross section is around 1000 nm, where the terminal laser level is separated from the fundamental pumping level by an energy difference only a few hundreds of cm^{-1} , corresponding to the thermal energy $k_B T$ at room temperature. Accordingly, thermal populating of the terminal laser level produces strong reabsorption losses and detrimentally affects the laser action. The second band around 1050 nm corresponds to an energy scheme of medium emission cross sections where the terminal level has a low population. Efficient laser action is possible. The last band around 1080 nm exhibits a terminal laser level with very low population but the emission cross section is very small. While in Yb:GSO, the emission band around 1088 nm not only exhibits a terminal laser level with very low population, but it also has the strongest emission cross section. In addition, although Yb^{3+} ions occupy two nonequivalent crystallographic sites in the GSO host matrix, the emission band around 1088 nm is related with Yb^{3+} ions in the site with larger crystal-field splitting, corresponding to a transition from the lowest sublevels of $^2F_{5/2}$ manifold to the highest sublevels of $^2F_{7/2}$ manifold. The energy difference between the fundamental pumping level and the terminal laser level is up to 1067 cm^{-1} , which is to the best of our knowledge the largest among ytterbium-doped crystals. At room temperature $T=300 \text{ K}$ (with the thermal energy $k_B T=208.5 \text{ cm}^{-1}$), the terminal laser level is populated with a probability of 6×10^{-3}

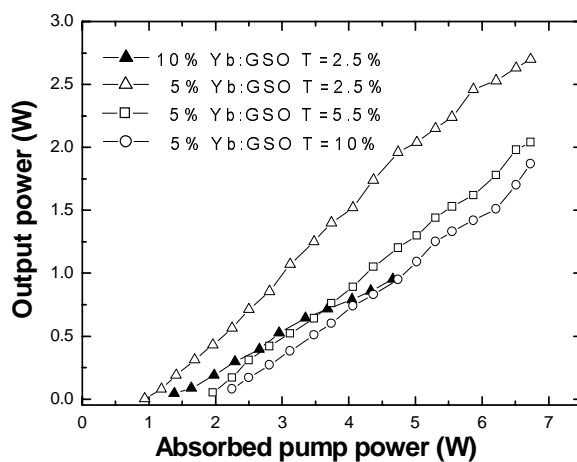


Fig. 4. Yb:GSO cw laser output power as a function of incident pump power.

according to the Boltzman thermal distribution. As a result, even without any intracavity wavelength selectors, Yb:GSO laser oscillates at a long wavelength depending on the laser crystal length and the transmission of the output coupler. In our cavity, as shown in Fig. 2, the Yb:GSO laser was operated near 1094 nm, which is the longest laser wavelength achieved for Yb³⁺ lasers.

Figure 4 presents the output power of cw Yb:GSO laser at 1094 nm as a function of the absorbed pump power. In order to optimize the laser efficiency, we compared the laser output with different output couplers of transmission T=2.5%, T=5.5% and T=10%, and Yb:GSO laser crystals with 5 at.% and 10 at.% Yb³⁺ doping. The maximum output power was obtained with the 5% doped crystal and T=2.5% output coupler. Under an absorbed pump power of 6.73 W (the incident pump power is 7.66 W), the output power reached 2.7 W. The corresponding slope efficiency was 49%. In contrast with Nd-doped materials, efficient cw laser action of 5 at.% and 10 at.% Yb:GSO indicates a capacity of high Yb-doping rate, without quenching by the cross-relaxation process.

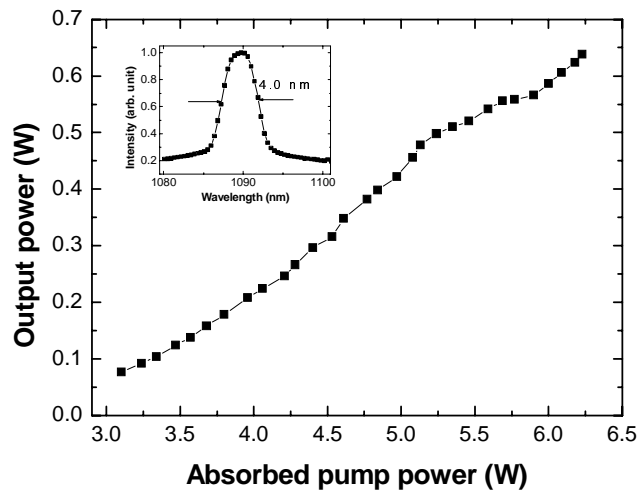


Fig. 5. CML Yb:GSO laser output power versus absorbed pump power and the corresponding laser spectrum (inset).

In the folded Yb:GSO laser resonator, as shown in Fig. 3, passive mode locking appears as the pump power reaches the threshold value of 3.2 W (absorbed pump power). It is well-known that Yb-doped materials move easily toward the Q-switched regime because of their long excited-state lifetimes. In our Yb:GSO laser, the strong tendency toward Q-switched mode locking was suppressed by choosing a proper intracavity laser beam spot-size diameter on the SESAM. CML rather than Q-switched mode-locking was observed even near the threshold pump. The laser cavity should be carefully aligned to reduce the mode-locking instability. Figure 5 shows that the average output power measured for the CML laser with a 2.5% output coupler as a function of the absorbed pump power. At a pump power of 6.23 W (the incident pump power is 7.12 W), a maximum average output power of 638 mW was obtained with a repetition rate of 145.5 MHz, corresponding to the laser energy 4.4 nJ per pulse, or 0.1 kW peak power. The corresponding slope efficiency was approximately 19% with respect to the absorbed pump power. The CML pulses were centered at 1089 nm with a spectral full-width of half-maximum (FWHM) about 4.0 nm. The spectral profile of the CML output pulses is shown in the inset of Fig. 5. Because of the presence of intense peaks, this bandwidth cannot be integrally used to generate short pulses. We recorded the output pulse train with a digital oscilloscope with 1 GHz bandwidth (Agilent 54833A DSO), as shown in

Fig. 6. The stability of the mode-locked operation was monitored by observing the output pulse train. After a careful cavity alignment, the CML Yb:GSO laser remained stable for hours, and the mode-locked pulse train showed no observable passive Q-switched envelopes. It was found that the CML operation was particularly sensitive to the alignment of SESAM. Figure 6 displays the power spectrum (Agilent E4411B) for the CML Yb:GSO laser. One can see that the CML laser is stable when operated at 145.5 MHz without sideband power spectra. The observed transversal mode structure of the Yb:GSO laser remained basically TEM₀₀ in both cw and passively mode-locked operation. The output pulse duration was measured with a homemade autocorrelator.

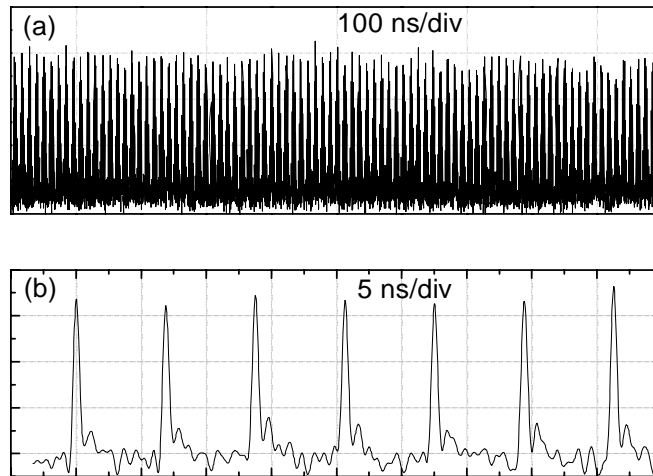


Fig. 6. (a) Pulse trains of the CML Yb:GSO laser. (b) The 145.5-MHz repetition rate of the CML pulses.

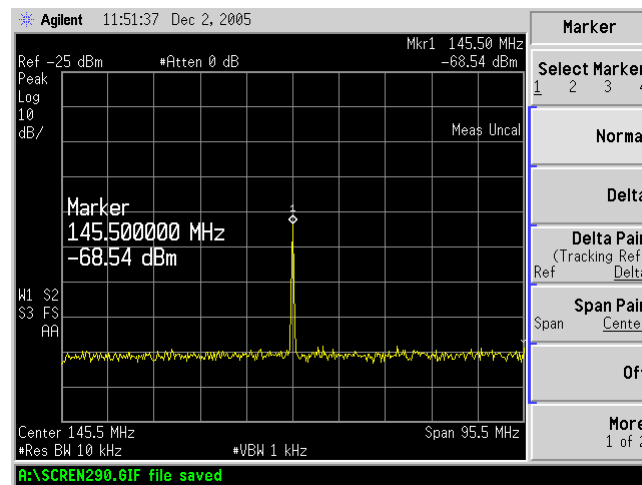


Fig. 7. Power spectrum of a CML Yb:GSO laser.

We obtained pulses as short as 46 ps (FWHM) assuming a Gaussian-shaped temporal intensity profile. The corresponding autocorrelation trace is shown in Fig. 8. According to the broad emission bandwidth of Yb:GSO, ultrashort pulses should be possible. Only picosecond

pulses were obtained in our experiments. This was probably caused by the group velocity dispersion, which was not compensated in the cavity.

In order to obtain a stable cw mode locking, the intracavity pulse energy E_P must exceed the Q-switched mode-locking threshold value determined by $E_P^2 > E_{sat,L} E_{sat,A} R$, where $E_{sat,A}$ and $E_{sat,L}$ denote the saturation energy of the absorber and gain medium, respectively, and R is the maximum change in nonlinear reflectivity, which is also referred to as the maximum modulation depth of the SESAM device. $E_{sat,L}$ is defined as the product of saturation fluence $F_{sat} = h\nu / (2\sigma_L)$ and the effective laser mode area inside the gain medium, where σ_L is the emission cross section. In the experiment, the threshold intracavity pulse energy for stable CML operation was measured as 10.5 nJ, which was much lower than the calculated E_P (831 nJ) with modulation depth of $R \sim 2\%$ and saturation fluence of $70 \mu\text{J}/\text{cm}^2$ (parameters of SESAM at the central wavelength 1064 nm). This implies that the SESAM used in our experiment might have smaller values of modulation depth and saturation fluence around the CML laser wavelength (1089 nm).

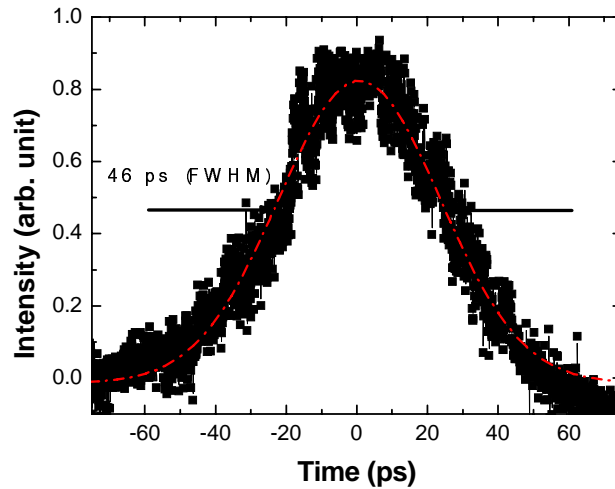


Fig. 8. Autocorrelation trace of the Yb:GSO CML laser.

5. Conclusions

In conclusion, we have demonstrated cw and cw mode-locked laser action of a new ytterbium-doped oxyorthosilicate crystal, Yb:GSO. In the cw laser operation regime, an output power of 2.7 W at 1094 nm was obtained at the pump power of 6.73 W by use of an output coupler of $T=2.5\%$. The corresponding slope efficiency was 49%. As compared with the 1082 nm Yb:YSO laser, the Yb:GSO laser at 1094 nm has, to the best of our knowledge, the longest laser wavelength achieved for Yb^{3+} lasers. We have also demonstrated for the first time to our knowledge picosecond pulse generation from a diode-pumped Yb:GSO laser passively mode locked with a SESAM. Laser pulses of 46 ps duration were obtained with an average output power of 638 mW and a repetition rate of 145.5 MHz. We believe that a femtosecond Yb:GSO laser can be realized with optimized laser cavity and mode-locking elements.

Acknowledgments

This work was partly supported by Key Project from the Science and Technology Commission of Shanghai Municipality (Grant Nos. 04dz14001 and 03XD14012), National Outstanding Youth Foundation (Grant Nos. 10525416 and 60425516), National Natural

Science Fund (Grant Nos. 10374028 and 60478011), and Key Project sponsored by the National Education Ministry of China (Grant No. 104193).